

# Geometry, Electronic Properties, and Hydrogen Adsorption Properties of $\text{Li}_3\text{N}$ -Based Nanostructures

Z. P. Jiang,<sup>†</sup> X. Zhou,<sup>†</sup> Qiang Sun,<sup>\*,†,‡</sup> Qian Wang,<sup>‡</sup> and Puru Jena<sup>‡</sup>

Department of Advanced Materials and Nanotechnology, and Center for Applied Physics and Technology, Peking University, Beijing 100871, China, and Department of Physics, Virginia Commonwealth University, Richmond, Virginia 23284, United States

Received: June 24, 2010; Revised Manuscript Received: August 13, 2010

Recent studies of hydrogen storage have focused on lithium metal atoms as dopants in a variety of substrates as Li is the lightest metallic element in the periodic table. In this work, we have explored the role of  $\text{Li}_3\text{N}$  nanostructures in hydrogen storage as they possess Li atoms with varying degrees of coordination. We have performed detailed calculations of geometries, electronic structures, and hydrogen adsorption properties of free  $(\text{Li}_3\text{N})_n$  ( $n = 1-7$ ) clusters and those supported on BN nanoribbons by using density functional theory and generalized gradient approximation for the exchange and correlation potential. We found general motifs of  $(\text{Li}_3\text{N})_n$  clusters where N sites form polygons for  $n \leq 4$  and polyhedrons  $n \geq 5$ . The binding energies per formula unit increase with size, whereas the HOMO–LUMO gaps decrease. The HOMO is mainly contributed by Li and the LUMO by N. The bonding between Li and N has both ionic and covalent character. Lithium sites with low coordination are found to have a stronger adsorption energy for hydrogen molecules, which varies in the range of 0.08–0.11 eV/ $\text{H}_2$ . When deposited on a BN nanoribbon, the  $\text{Li}_3\text{N}$  molecules show stronger adsorption of hydrogen due to the changes in charge distribution. This suggests that  $\text{Li}_3\text{N}$  molecules or small clusters can be introduced in porous substrates for enhancing hydrogen storage.

## 1. Introduction

Hydrogen is considered to be a potential alternative to fossil fuels for applications in the mobile industry. However, the ability to store hydrogen with large gravimetric and volumetric densities and to operate the storage devices at near ambient thermodynamic conditions is vital to the success of the hydrogen economy. No suitable storage materials are yet available. Hydrogen is bound either strongly, as in light metal hydrides, or weakly, as in metallo-organic frameworks (MOFs), making their operation at room temperature and pressure very difficult. In the former, hydrogen atoms are bound dissociatively and are held together with strong covalent or ionic bonds between hydrogen and metal atoms. In the later, hydrogen atoms bind molecularly. An intermediate form of binding where hydrogen atoms are bound quasi-molecularly is showing a lot of promise in the design and synthesis of hydrogen storage materials. In this regard, considerable efforts are being made in studying the interaction of nanostructured materials with hydrogen.

Recently, Bhatia and Myers<sup>1</sup> studied the optimum thermodynamic conditions for hydrogen adsorption, employing the Langmuir equation and derived relationships between the operating pressure of a storage tank and the enthalpy of adsorption required for storage near room temperature. They have found that the average optimal adsorption enthalpy should be in the range of 0.1–0.2 eV/ $\text{H}_2$ . To reach this energy window as well as the gravimetric density of hydrogen of the D.O.E.'s 6 wt % target, the use of Li metal has many advantages. One of the widely used strategies is to introduce lithium to various substrates, such as fullerene cages, nanotubes, graphene sheets,

and MOFs.<sup>2–12</sup> It has been found that lithium can significantly enhance the adsorption of hydrogen molecules. However, it is technically not easy to introduce metal ions to substrates without clustering.<sup>13</sup> It will be ideal if metal ions can be incorporated into a material in a natural way such that they can be prevented from clustering while still maintaining their ability to trap hydrogen in quasi-molecular form. In particular, it will be ideal if these metal centers form the intrinsic backbone of the storage material.  $\text{Li}_3\text{N}$  is such a system, where separated Li ions form the backbone. We note that, in  $\text{Li}_3\text{N}$ , the charge transfer from Li to N keeps the Li atoms in a positively charged state. Thus, the Li atoms in  $\text{Li}_3\text{N}$  can bind hydrogen in molecular form. Studies have been carried out using the  $\text{Li}_3\text{N}$  surface for hydrogen storage,<sup>14</sup> where the available Li sites are only at the surface, whereas inside the bulk, there is no space for the adsorption of hydrogen molecules. To increase the number of Li sites for the adsorption, nanostructures can be used, where more Li sites are exposed, thus providing the possibilities for hydrogen adsorption. Here, three basic questions arise: What are the equilibrium geometries of  $(\text{Li}_3\text{N})_n$ ? How strong is the adsorption of hydrogen molecules in these nanostructures? How can we assemble the  $\text{Li}_3\text{N}$  molecule for a better hydrogen storage performance? In this paper, we have addressed these questions by studying the geometry, electronic structures, and the adsorption of  $\text{H}_2$  in free and supported  $\text{Li}_3\text{N}$ -based nanostructures.

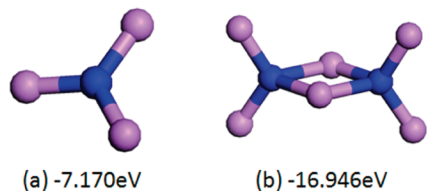
## 2. Computational Method

Our calculations are based on an all-electron density functional theory (DFT) with the generalized gradient approximation (GGA) for the exchange and correlation potential. For the later, we have used the PW91<sup>15</sup> functional as implemented in the DMol3 package.<sup>16,17</sup> Double numerical polarized (DNP) basis sets are employed. All the atoms are relaxed without any symmetry constraints. Convergence in energy, force, and

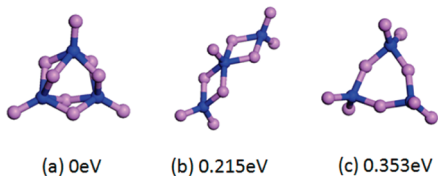
\* To whom correspondence should be addressed. E-mail: sunqiang@pku.edu.cn.

<sup>†</sup> Peking University.

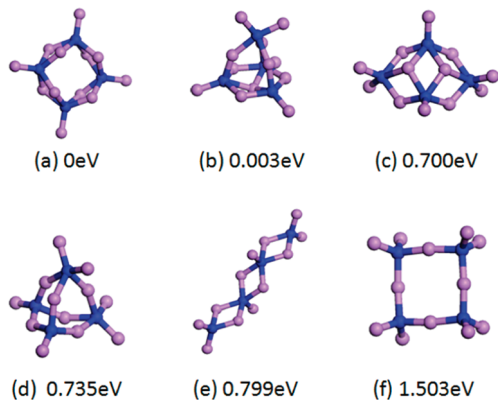
<sup>‡</sup> Virginia Commonwealth University.



**Figure 1.** Geometry and the binding energy for Li<sub>3</sub>N (a) and (Li<sub>3</sub>N)<sub>2</sub> (b).



**Figure 2.** Geometry and the relative energy for (Li<sub>3</sub>N)<sub>3</sub> isomers.

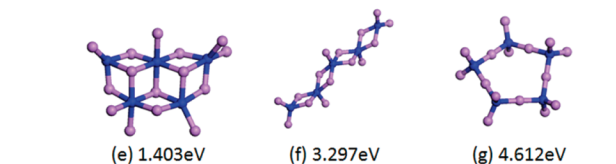
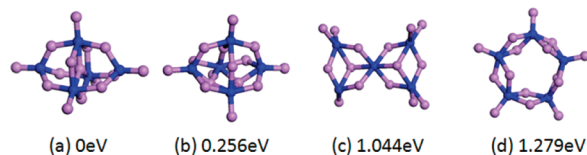


**Figure 3.** Geometry and the relative energy for (Li<sub>3</sub>N)<sub>4</sub> isomers.

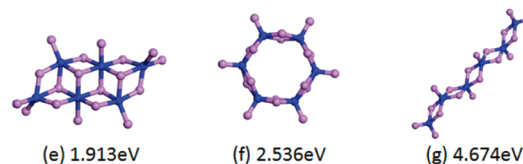
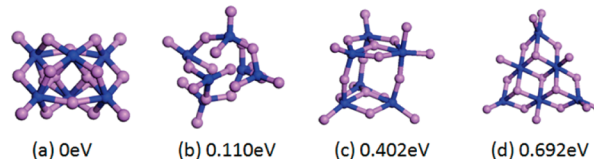
displacement was set at  $2 \times 10^{-5}$  Ha, 0.001 Ha/Å, and 0.005 Å, respectively. The accuracy of our exchange–correlation functional and basis set was tested with the following data. The bond length and binding energy of H<sub>2</sub>, Li<sub>2</sub>, and N<sub>2</sub> molecules are calculated to be 0.75 Å (4.557 eV), 2.71 Å (0.834 eV), and 1.11 Å (10.286 eV), respectively, which agree well with the corresponding experimental values<sup>18</sup> of 0.741 Å (4.45 eV), 2.67 Å (1.10 eV), and 1.10 Å (9.45 eV).

### 3. Results and Discussion

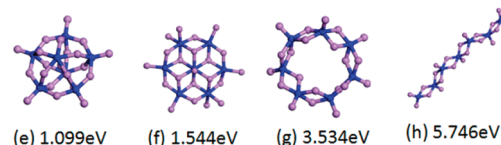
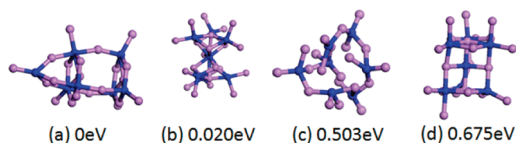
The geometry of the Li<sub>3</sub>N monomer is a planar structure with *D*<sub>3h</sub> symmetry (Figure 1a). The dimer of (Li<sub>3</sub>N)<sub>2</sub> can be built using two Li atoms, forming a double bridge (DB) where two N atoms are bound (Figure 1b) or using a single bridge (SB) where the Li atom in one Li<sub>3</sub>N unit binds to a N atom in the other. After optimization, we find that the latter changes to the former, resulting in a DB structure as the ground-state geometry. For (Li<sub>3</sub>N)<sub>3</sub>, we have three possible structures: a DB ring (Figure 2a), a DB chain (Figure 2b), and an SB ring (Figure 2c). The structure optimization shows that the DB ring structure has the lowest energy. For (Li<sub>3</sub>N)<sub>4</sub>, besides the chain, SB, and DB structures, we consider another three isomers, as shown in Figure 3. On the basis of the relative energy, we find that the DB ring structure in Figure 3a and the one with a tetrahedron skeleton (Figure 3b) are energetically degenerate, whereas the DB chain and the SB ring structures are much higher in energy. For (Li<sub>3</sub>N)<sub>5</sub>, the structure with the lowest energy is found to be an N-site based triangle bipyramid (Figure 4a). The DB ring is 1.28 eV higher in energy, and the SB ring is metastable and is 2.33 eV higher in energy than the DB ring. For (Li<sub>3</sub>N)<sub>6</sub>, the SB ring is unstable. The optimized structure (Figure 5b) is similar



**Figure 4.** Geometry and the relative energy for (Li<sub>3</sub>N)<sub>5</sub> isomers.



**Figure 5.** Isomers and the relative energy for (Li<sub>3</sub>N)<sub>6</sub>.



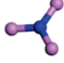

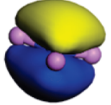
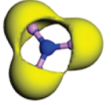
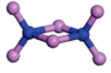

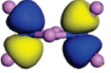
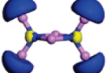
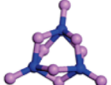

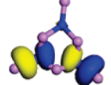
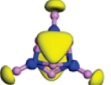
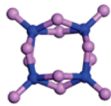

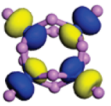
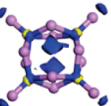
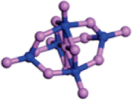

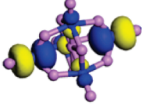
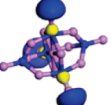
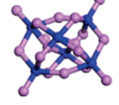

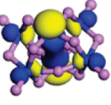
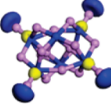
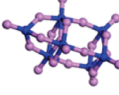

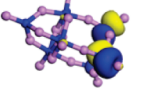
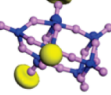
**Figure 6.** Isomers and the relative energy for (Li<sub>3</sub>N)<sub>7</sub>.

to the ground-state geometry (Figure 5a), where the six N sites consist of a prism skeleton, whereas the DB ring is 2.54 eV higher in energy. The ground-state geometry of (Li<sub>3</sub>N)<sub>7</sub> (Figure 6a) can be obtained from (Li<sub>3</sub>N)<sub>6</sub> by capping one Li<sub>3</sub>N, namely, the seven N sites consist of a capped prism skeleton.

On the basis of the above results, we can see the following general trend in geometries of (Li<sub>3</sub>N)<sub>*n*</sub> clusters: (1) For *n* = 3 and 4, the SB ring structure is metastable, whereas for *n* = 5, 6, and 7, it becomes unstable. The backbone of the SB ring structure cannot be maintained upon optimization. (2) The DB ring and DB chain are metastable for the clusters studied. As the size increases, the strain in the DB ring becomes less and the energy becomes more favorable as compared with the DB chain. (3) The DB ring structure can be viewed as a N-site based 2D geometry. Beginning with (Li<sub>3</sub>N)<sub>5</sub>, the DB structure becomes a higher energy isomer and the ground-state geometry tends to be a 3D N-site based polyhedron, for example, a trianglular bipyramid (*n* = 5), a prism (*n* = 6), and a prism pyramid (*n* = 7).

In Table 1, we summarize the main results for the low-energy states, including geometry, the skeleton of N sites, the HOMO, the LUMO, the energy gap, and the average binding energy per unit. We note that the HOMOs are mainly contributed by

**TABLE 1: Geometry, Electronic Structures, Average Binding Energy per Li<sub>3</sub>N Unit (BE/*n*, in eV), and the HOMO–LUMO Gap ( $\Delta$ , in eV) of (Li<sub>3</sub>N)<sub>*n*</sub> Clusters Corresponding to Their Lowest-Energy Configuration**

Size	Structures	N-skeleton	HOMO	LUMO	BE/ <i>n</i>	$\Delta$
<i>n</i> =1					-7.170	1.198
<i>n</i> =2					-8.473	1.238
<i>n</i> =3					-9.120	1.133
<i>n</i> =4					-9.450	0.872
<i>n</i> =5					-9.822	0.983
<i>n</i> =6					-10.019	0.930
<i>n</i> =7					-10.113	0.892

N sites and the LUMOs are by Li sites, similar to what happens in bulk Li<sub>3</sub>N where the valence band is composed of N 2s and N 2p, whereas the conduction band is composed of Li 2s.<sup>19</sup> The changes in the HOMO–LUMO gap are not very sensitive to the size. From *n* = 1 to *n* = 2, it varies from 1.2 to 1.1 eV, whereas from *n* = 3 to *n* = 7, it changes in the range of 0.8–0.9 eV, while the average binding energy per unit increases and approaches a saturated value of about 10 eV.

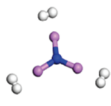
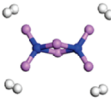
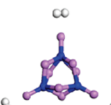
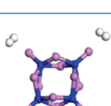
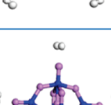
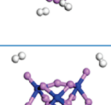
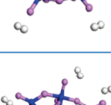
According to the geometries listed in Table 1, we can see that the Li atoms behave like ligands on N sites. There are two kinds of Li atoms: the top and the bridge site of N. Charge analysis indicates that, in (Li<sub>3</sub>N)<sub>*n*</sub> clusters, charge transfer between Li and N is small, and the bonding is partially ionic and partially covalent. The Li at the top site carries more charges (about 0.24–0.27 electrons) than that in the bridge site (about 0.1–0.15 electrons). These partially charged Li ions produce a local electric field that can polarize hydrogen molecules for enhancing their adsorption energies. In the following, we discuss hydrogen adsorption on (Li<sub>3</sub>N)<sub>*n*</sub> clusters.

For Li<sub>3</sub>N, there are three Li ions on the top site. When a hydrogen molecule is introduced to each site, the adsorption energy is found to be 0.11 eV. For (Li<sub>3</sub>N)<sub>2</sub>, there are four Li ions on the top site, each adsorbing one H<sub>2</sub> with a binding energy of 0.11 eV. For Li ions on the bridge site, the adsorption is much weaker (0.045 eV) because it carries less charges. For our discussions below, we focus on H<sub>2</sub> adsorption on the top

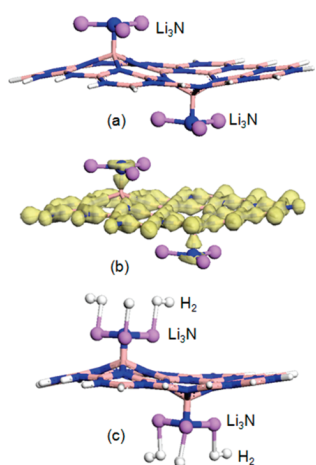
site. In (Li<sub>3</sub>N)<sub>*n*</sub> with *n* = 3–7, the corresponding number of top-site Li ions is 3, 4, 5, 6, and 7, respectively, and the adsorption energy is found to be 0.093, 0.094, 0.097, 0.096, and 0.123 eV/H<sub>2</sub>, as shown in Table 2. This table also contains detailed information, including the bond length and charges. Therefore, the average adsorption energy on the top-site Li ions is about 0.1 eV, which is close to the desirable energy window for applications.

On the basis of the above results, we note that, when Li<sub>3</sub>N is used as a building block, the number of Li ions on the bridge sites increases with size. The adsorption energy and the gravimetric density get smaller. Therefore, assembling Li<sub>3</sub>N molecules to form larger nanoparticles does not provide a promising pathway for hydrogen storage. To avoid Li's from binding with each other, one can deposit Li<sub>3</sub>N molecules on substrates with large surface areas, such as other nanomaterials and porous materials. We have chosen a BN nanoribbon to demonstrate this possibility because a single atomic BN layer has already been successfully synthesized,<sup>20</sup> and unlike a graphene sheet, the BN sheet has an ionic bonding feature between B and N, where the positively charged B site can bind with the negatively charged N site in the Li<sub>3</sub>N molecule. To balance the interaction, we deposited one Li<sub>3</sub>N unit on each side of the BN nanoribbon. Optimization shows that this absorption causes local distortions in geometry, as shown in Figure 7a. The distance between Li<sub>3</sub>N and the nanoribbon is

**TABLE 2: Average Distance between Li and H<sub>2</sub> ( $d_{\text{H}_2-\text{Li}}$ , in Å), the Average Adsorption Energy per H<sub>2</sub> (AE/H<sub>2</sub>, in eV), and the Average Charge on Each Top-Site Li Ion ( $Q$ , in Electrons) in the (Li<sub>3</sub>N)<sub>*n*</sub> Clusters with Adsorbed Hydrogen Molecules**

Size	Structures	$D_{\text{H}_2-\text{Li}}$	BE/H <sub>2</sub>	Q
n=1		2.085	0.110	0.262
n=2		2.088	0.106	0.266
n=3		2.121	0.093	0.240
n=4		2.123	0.094	0.257
n=5		2.104	0.097	0.246
n=6		2.125	0.096	0.239
n=7		2.083	0.123	0.242

1.507 Å, and the interaction energy is found to be 2.11 eV per Li<sub>3</sub>N unit. To understand the bonding feature between Li<sub>3</sub>N



**Figure 7.** Geometry (a), electron density with a value of 0.26 electrons/Å<sup>3</sup> (b), and hydrogen adsorption (c) of Li<sub>3</sub>N deposited on a BN nanoribbon.

molecules and the substrates, we plotted the charge distribution isosurface in Figure 7b. This indicates that the interaction is mainly covalent. The interesting observation is that Li sites carry more charges (0.32) when deposited on the substrate than when they are in the free state, namely, 0.26. The mechanism involved in charge transfer is the following: When deposited on the substrate, the N site in Li<sub>3</sub>N shares its electrons with the B site in the substrate, thus reducing the electron sharing of the N site with Li sites. This relatively increases the ionic bonding. This is confirmed from the increase of the Li–N bond length (from 1.73 to 1.80 Å). The charged Li ions produce a local electric field that polarizes H<sub>2</sub> molecules, hence resulting in enhanced adsorption. In fact, we found the adsorption energy to be 0.12 eV/H<sub>2</sub>, stronger than the adsorption in free state. This finding is quite encouraging, as it shows that introduction of Li<sub>3</sub>N molecules to substrates, such as MOFs and COFs, can lead to enhancement in hydrogen sorption.

#### 4. Conclusions

In summary, we have explored the possibility that Li atoms in nanostructured Li<sub>3</sub>N can be used for hydrogen storage. We calculated the geometry and electronic properties of (Li<sub>3</sub>N)<sub>*n*</sub> clusters and found that, as the cluster size increases, the coordination of Li ions increases, leading to a weakening of hydrogen adsorption. On the other hand, as Li<sub>3</sub>N molecules are deposited on a substrate, the changes in charge distributions make Li more ionic, which, in turn, leads to an increase in hydrogen adsorption energy. This provides a new strategy to improve the properties of materials for hydrogen storage.

**Acknowledgment.** This work is partially supported by grants from the National Natural Science Foundation of China (10874007 and 20973010), the National Grand Fundamental Research 973 Program of China (2010CB631301), and by the U.S. Department of Energy.

#### References and Notes

- (1) Bhatia, S.; Myers, A. L. *Langmuir* **2006**, *22*, 1688.
- (2) Niu, J.; Rao, B. K.; Jena, P. *Phys. Rev. Lett.* **1992**, *68*, 2277.
- (3) Rao, B. K.; Jena, P. *Europhys. Lett.* **1992**, *20*, 307.
- (4) Niu, J.; Rao, B. K.; Jena, P.; Manninen, M. *Phys. Rev. B* **1995**, *51*, 4475.
- (5) Sun, Q.; Jena, P.; Wang, Q.; Marquez, M. *J. Am. Chem. Soc.* **2006**, *128*, 9741.
- (6) Sun, Q.; Wang, Q.; Jena, P. *Appl. Phys. Lett.* **2009**, *94*, 013111.
- (7) Wu, X.; Gao, Y.; Zeng, X. C. *J. Phys. Chem. C* **2008**, *112*, 8458.
- (8) Liu, W.; Zhao, Y. H.; Li, Y.; Jiang, Q.; Lavernia, E. J. *J. Phys. Chem. C* **2009**, *113*, 2028.
- (9) Du, A.; Zhu, Z.; Smith, S. C. *J. Am. Chem. Soc.* **2010**, *132*, 2876.
- (10) Yang, S.; Lin, X.; Blake, A. J.; Walker, G. S.; Hubberstey, P.; Champness, N. R.; Schroder, M. *Nat. Chem.* **2009**, *1*, 487.
- (11) Klontzas, E.; Mavrandonakis, A.; Tyliaakis, E.; Froudakis, G. E. *Nano Lett.* **2008**, *8*, 1572.
- (12) Mavrandonakis, A.; Tyliaakis, E.; Stubos, A. K.; Froudakis, G. E. *J. Phys. Chem. C* **2008**, *112*, 7290.
- (13) Sun, Q.; Wang, Q.; Jena, P.; Kawazoe, Y. *J. Am. Chem. Soc.* **2005**, *127*, 14582.
- (14) Jin, H. M.; Luo, J. Z.; Wu, P. *Appl. Phys. Lett.* **2007**, *90*, 084101.
- (15) Wang, Y.; Perdew, J. P. *Phys. Rev. B* **1991**, *44*, 13298.
- (16) Delley, B. *J. Chem. Phys.* **1990**, *92*, 508.
- (17) Delley, B. *J. Chem. Phys.* **2000**, *113*, 7756.
- (18) Lide, D. R., Ed. *CRC Handbook of Chemistry and Physics*; CRC Press: New York, 2000.
- (19) Zhao, Y.; Tian, X.; Xue, W.; Gao, T. *Solid State Commun.* **2009**, *149*, 2130.
- (20) Han, W. Q.; Wu, L.; Zhu, Y.; Watanabe, K.; Taniguchi, T. *Appl. Phys. Lett.* **2008**, *93*, 223103.